NASA TECHNICAL NOTE

NASA TN D-8267

NASA TN D-8267

THE EFFECT OF WINGLETS ON THE STATIC AERODYNAMIC STABILITY CHARACTERISTICS OF A REPRESENTATIVE SECOND GENERATION JET TRANSPORT MODEL

Peter F. Jacobs and Stuart G. Flechner

Langley Research Center
Hampton, Va. 23665

NATIONAL AERONAUTICS AND SPACE ADMINISTRATION • WASHINGTON, D. C. • JULY 1976

1. Report No.	2. Government Accession No.	3. Recipient's Catalog No.
NASA TN D-8267		

4. Title and Subtitle
THE EFFECT OF WINGLETS ON THE STATIC AERODYNAMIC STABILITY CHARACTERISTICS OF A REPRESENTATIVE SECOND GENERATION JET TRANSPORT MODEL

5. Report Date: July 1976

6. Performing Organization Code:

7. Author(s)
Peter F. Jacobs and Stuart G. Flechner

8. Performing Organization Report No.: L-10297

9. Performing Organization Name and Address
NASA Langley Research Center
Hampton, Va. 23665

10. Work Unit No.: 505-11-11-04

11. Contract or Grant No.:

12. Sponsoring Agency Name and Address
National Aeronautics and Space Administration
Washington, D.C. 20546

13. Type of Report and Period Covered: Technical Note

14. Sponsoring Agency Code:

15. Supplementary Notes:

16. Abstract

This investigation was made to determine the effects of winglets on the static aerodynamic stability characteristics of a full-span representative second generation jet transport model without tails. Two configurations were tested: a baseline wing and a version of the same wing fitted with winglets. The longitudinal aerodynamic characteristics were determined through an angle-of-attack range from -1° to 10° at an angle of sideslip of 0° for Mach numbers of 0.750, 0.800, and 0.825. The lateral aerodynamic characteristics were determined through the same angle-of-attack range at fixed sideslip angles of 2.5° and 5°. Both configurations were investigated at Reynolds numbers of 13×10^6 per meter (4×10^6 per foot) and approximately 20×10^6 per meter (6×10^6 per foot).

The winglet configuration showed slight increases over the baseline wing in static longitudinal and lateral aerodynamic stability throughout the test Mach number range for a model design lift coefficient of 0.53. Reynolds number variation had very little effect on stability.

17. Key Words (Suggested by Author(s))	18. Distribution Statement
Winglets Induced drag Drag due to lift Stability	Unclassified – Unlimited Subject Category 02

19. Security Classif. (of this report)	20. Security Classif. (of this page)	21. No. of Pages	22. Price*
Unclassified	Unclassified	30	$3.75

*For sale by the National Technical Information Service, Springfield, Virginia 22161

THE EFFECT OF WINGLETS ON THE STATIC AERODYNAMIC STABILITY CHARACTERISTICS OF A REPRESENTATIVE SECOND GENERATION JET TRANSPORT MODEL

Peter F. Jacobs and Stuart G. Flechner
Langley Research Center

SUMMARY

This investigation was made to determine the effects of winglets on the static aerodynamic stability characteristics of a full-span representative second generation jet transport model without tails. Two configurations were tested: a baseline wing and a version of the same wing fitted with winglets. The longitudinal aerodynamic characteristics were determined through an angle-of-attack range from -1° to 10° at an angle of sideslip of 0° for Mach numbers of 0.750, 0.800, and 0.825. The lateral aerodynamic characteristics were determined through the same angle-of-attack range at fixed sideslip angles of 2.5° and 5°. Both configurations were investigated at Reynolds numbers of 13×10^6 per meter (4×10^6 per foot) and approximately 20×10^6 per meter (6×10^6 per foot).

The winglet configuration showed slight increases over the baseline wing in static longitudinal and lateral aerodynamic stability throughout the Mach number range for a model design lift coefficient of 0.53. Reynolds number variation had very little effect on stability.

INTRODUCTION

Winglets, described in reference 1, are intended to provide reductions in drag coefficient for near-cruise conditions substantially greater than those obtained with simple wing-tip extensions which impose the same bending increments on the wing structure. The National Aeronautics and Space Administration has been conducting extensive experimental investigations of the effects of winglets for jet transport wings at high subsonic Mach numbers.

This investigation was conducted to determine the effects of winglets on the lateral-directional and longitudinal aerodynamic stability characteristics of a full-span transport model without tails for cruise Mach numbers of 0.750, 0.800, and 0.825. To observe the sensitivity of the model stability parameters to Reynolds number, tests were conducted at

two different Reynolds numbers: 13×10^6 per meter (4×10^6 per foot) and approximately 20×10^6 per meter (6×10^6 per foot). This stability analysis, presented at a wing-body lift coefficient of 0.53, corresponds to the somewhat lower overall cruise lift coefficient of a typical transport aircraft having a downward-loaded horizontal tail.

The nature of this investigation necessitated a strain-gage balance capable of measuring large forces and moments. Unfortunately, the relatively large axial-force beam of this balance was insufficiently accurate to measure the small increments of drag involved in this investigation. Even if it were possible to measure these drag increments, the test Reynolds numbers of the winglets (approximately 0.4×10^6 and 0.6×10^6 based on average chord, for the upper winglet) are so low that the winglets experience disproportionately large skin-friction drag levels. For these reasons, accurate absolute values of drag are unobtainable; therefore, drag data are not given in this report. (Drag data are presented in ref. 2.)

SYMBOLS

The results presented in this report are referred to the stability-axis system for the longitudinal aerodynamic characteristics and to the body-axis system for the lateral-directional aerodynamic characteristics. Force and moment data have been reduced to conventional coefficient form based on the geometry of the baseline wing planform. Moments are referenced to the quarter-chord point of the mean aerodynamic chord of the baseline wing (fig. 1). All dimensional values are given in both the International System of Units (SI) (ref. 3) and U.S. Customary Units; however, all measurements and calculations were made in U.S. Customary Units.

Coefficients and symbols used herein are defined as follows:

b	wing span, 114.45 cm (45.06 in.)
C_L	lift coefficient, $\frac{\text{Lift}}{qS}$
C_{L_α}	lift-curve slope per degree, $\frac{\partial C_L}{\partial \alpha}$
C_l	rolling-moment coefficient (C_l on computer-drawn figures), $\frac{\text{Rolling moment}}{qSb}$
C_{l_β}	rate of change of rolling-moment coefficient with sideslip angle (effective-dihedral parameter) $\frac{\Delta C_l}{\Delta \beta}$, per degree
C_m	pitching-moment coefficient, $\frac{\text{Pitching moment}}{qS\bar{c}}$

$C_{m_{C_L}}$ longitudinal stability derivative, $\frac{\partial C_m}{\partial C_L}$

$C_{m,o}$ pitching-moment coefficient at zero lift

C_n yawing-moment coefficient, $\frac{\text{Yawing moment}}{qSb}$

C_{n_β} rate of change of yawing-moment coefficient with sideslip angle (directional-stability parameter) $\frac{\Delta C_n}{\Delta \beta}$, per degree

C_Y side-force coefficient, $\frac{\text{Side force}}{qS}$

C_{Y_β} rate of change of side-force coefficient with sideslip angle (side-force parameter) $\frac{\Delta C_Y}{\Delta \beta}$, per degree

c local streamwise chord of wing

$\bar{c}$ mean aerodynamic chord of baseline reference wing panel, 18.06 cm (7.11 in.)

M free-stream Mach number

q free-stream dynamic pressure, N/m^2 (psf)

R Reynolds number per unit length, per m (per ft)

S baseline wing planform reference area, 0.1884 m^2 (2.028 ft^2)

α angle of attack, deg

β angle of sideslip, deg

Δ values obtained by interpolation

∂ values obtained by linear regression

APPARATUS AND PROCEDURES

Model Description

A full-span, sting-mounted transport model without tails was used in this investigation (fig. 1). The model has a relatively wide cylindrical fuselage similar to present

second generation jet transports and a conventional low wing with 3° of incidence and $6^{\circ}40'$ of twist (washout) distributed nonlinearly between the root and tip chords. The wing has an aspect ratio of 6.95, a taper ratio of 0.299, and 35° of sweep at the quarter chord. The thickness ratio of the wing varies from 0.124 at the wing-fuselage juncture to 0.09 at midsemispan; this ratio then remains a constant 0.09 out to the tip.

A variation of this baseline configuration was also tested. The outboard 1.91 cm (0.75 in.) of the wing was removed and two winglets were installed on each wing tip. The two winglets, one large inclined upward and one small inclined downward, have trapezoidal planforms with a supercritical airfoil section (fig. 1).

The total winglet area represents 2.75 percent of the total wing area. The trailing edges of the upper winglets and the wing tips were flush mounted with the winglets canted outboard 15° from vertical (75° dihedral) and toed-out 2° relative to the fuselage center line.

Similarly, the leading edges of the lower winglets and the wing tips were also flush mounted with the winglets canted outboard 40° from vertical (50° anhedral) and toed-in 5° relative to the fuselage center line.

Test Facility

The investigation was conducted in the Langley 8-foot transonic pressure tunnel, a continuous, single-return tunnel with a slotted, rectangular test section. The longitudinal slots in the floor and ceiling of the test section reduce wall interference effects and allow relatively large models to be tested through the subsonic speed range. Available controls permit independent variation of Mach number, stagnation pressure and temperature, and dewpoint. A more detailed description of the tunnel is found in reference 4.

Test Conditions

Measurements were taken at Mach numbers of 0.750, 0.800, and 0.825 for an angle-of-attack range of -1° to 10° and nominal sideslip angles of 0°, 2.5°, and 5°. The Reynolds numbers and dynamic pressures at which the data were taken are presented in table I. Stagnation temperature was maintained at 322 K (120° F) and the air was dried until the dewpoint was sufficiently low to prevent condensation effects.

Boundary-Layer Transition

For all test Mach numbers, boundary-layer transition strips were sized and located by using the techniques discussed in references 5 and 6 to simulate the boundary-layer and shock-induced separation characteristics at a typical full-scale transport Reynolds number of 40×10^6.

A boundary-layer transition strip of No. 180 carborundum grains (set in a plastic adhesive) was applied to the fuselage 3.81 cm (1.50 in.) aft of the nose. On the winglets, transition strips of No. 220 carborundum grains were applied 0.25 cm (0.10 in.) from the leading edge of each upper surface and at 40 percent of the streamwise chord on each lower surface. The transition strips on the upper surface of the winglets were located forward in order to eliminate interaction of a shock wave and the laminar flow (based on previous experience with this model). (The transition pattern on the wing is shown in fig. 2. All transition strips were 0.16 cm (0.06 in.) wide.)

The fluorescent-oil film flow visualization technique described in reference 7 was employed to verify the presence of laminar flow ahead of the transition strip.

Measurements

Force and moment data were obtained by use of a six-component electrical strain-gage balance housed within the fuselage cavity. Drag data, for the reasons previously stated, are not presented. Angle of attack was measured by an accelerometer that was also housed within the fuselage. Static pressures were measured in the model along the sting cavity by using differential-pressure transducers referenced to free-stream static pressures.

Corrections

The angle of attack of the model was corrected for flow angularity in the tunnel test section. This correction was obtained from upright and inverted tests of the baseline wing configuration. The lift and pitching-moment coefficients have been adjusted to correspond to the condition of free-stream static pressure in the sting cavity. Blockage and interference effects were negligible; therefore, no corrections to the data have been made for these factors.

PRESENTATION OF RESULTS

The results of this investigation are presented in the following figures:

DISCUSSION

Longitudinal Aerodynamic Characteristics

The static longitudinal aerodynamic characteristics of the model with and without winglets are presented in figure 3 and summarized in figure 4 for the two test Reynolds numbers.

Although the actual variation of absolute values of C_m at all test conditions (fig. 3) is nearly negligible, the winglets do provide small increases in longitudinal stability (fig. 4). These increases are shown by more negative $C_{m_{C_L}}$ values. (Note that the $C_{m_{C_L}}$ values become increasingly negative with Mach number and that the difference between the curves for winglets on and off remains fairly constant over the test Mach number range.) This increased stability trend is offset somewhat by an increasing zero-lift pitching-moment coefficient. A very slight positive effect on the longitudinal stability characteristics due to increased Reynolds number is shown.

Lateral Aerodynamic Characteristics

A summary of the static lateral-directional aerodynamic characteristics of the model is presented in figure 6. Although the absolute values of these stability parameters are small (as in the longitudinal case), the winglets do have a slight positive effect on each of the lateral-directional stability parameter levels. Although the actual winglet Reynolds numbers are small, a slight positive effect is again shown on the stability parameters at the higher test Reynolds numbers.

CONCLUDING REMARKS

An investigation was made at Mach numbers of 0.750, 0.800, and 0.825 of the static longitudinal and lateral aerodynamic characteristics of a tailless full-span representative transport model with and without winglets.

Winglets were initially proposed to be retrofitted to existing aircraft to reduce induced drag. The results of this investigation showed that no adverse stability penalties could be attributed to the addition of winglets; in fact, the winglets actually showed small positive increases in both lateral and longitudinal stability over the baseline configuration.

Although the winglet Reynolds numbers were quite low, there was a very slight positive effect on the stability parameters at the higher test Reynolds number. Experience suggests that the stability benefits exhibited by winglets will continue to increase with further increases in Reynolds number.

Increases in the directional stability of an aircraft utilizing winglets presented the possibility of reducing the vertical tail surface, with a resulting decrease in drag.

Langley Research Center
National Aeronautics and Space Administration
Hampton, Va. 23665
May 19, 1976

REFERENCES

1. Whitcomb, Richard T.: A Design Approach and Selected Wind-Tunnel Results at High Subsonic Speed for Wing-Tip Mounted Winglets. NASA TN D-8260, 1976.

2. Flechner, Stuart G.; Jacobs, Peter F.; and Whitcomb, Richard T.: A High Subsonic Speed Wind-Tunnel Investigation of Winglets on a Representative Second-Generation Jet Transport Wing. NASA TN D-8264, 1976.

3. Mechtly, E. A.: The International System of Units – Physical Constants and Conversion Factors. NASA SP-7012, 1973.

4. Schaefer, William T., Jr.: Characteristics of Major Active Wind Tunnels at the Langley Research Center. NASA TM X-1130, 1965.

5. Braslow, Albert L.; and Knox, Eugene C.: Simplified Method for Determination of Critical Height of Distributed Roughness Particles for Boundary-Layer Transition at Mach Numbers From 0 to 5. NACA TN 4363, 1958.

6. Blackwell, James A., Jr.: Preliminary Study of Effects of Reynolds Number and Boundary-Layer Transition Location on Shock-Induced Separation. NASA TN D-5003, 1969.

7. Loving, Donald L.; and Katzoff, S.: The Fluorescent-Oil Film Method and Other Techniques for Boundary-Layer Flow Visualization. NASA MEMO 3-17-59L, 1959.

TABLE I.- SUMMARY OF TEST CONDITIONS

M	R		q	
	per m	per ft	kN/m^2	psf
0.750	13.12×10^6	4.00×10^6	30.14	629.55
	19.91×10^6	6.07×10^6	45.82	957.07
0.800	13.12×10^6	4.00×10^6	31.58	659.51
	20.57×10^6	6.27×10^6	49.96	1043.34
0.825	13.12×10^6	4.00×10^6	32.28	674.22
	21.00×10^6	6.40×10^6	51.81	1082.04

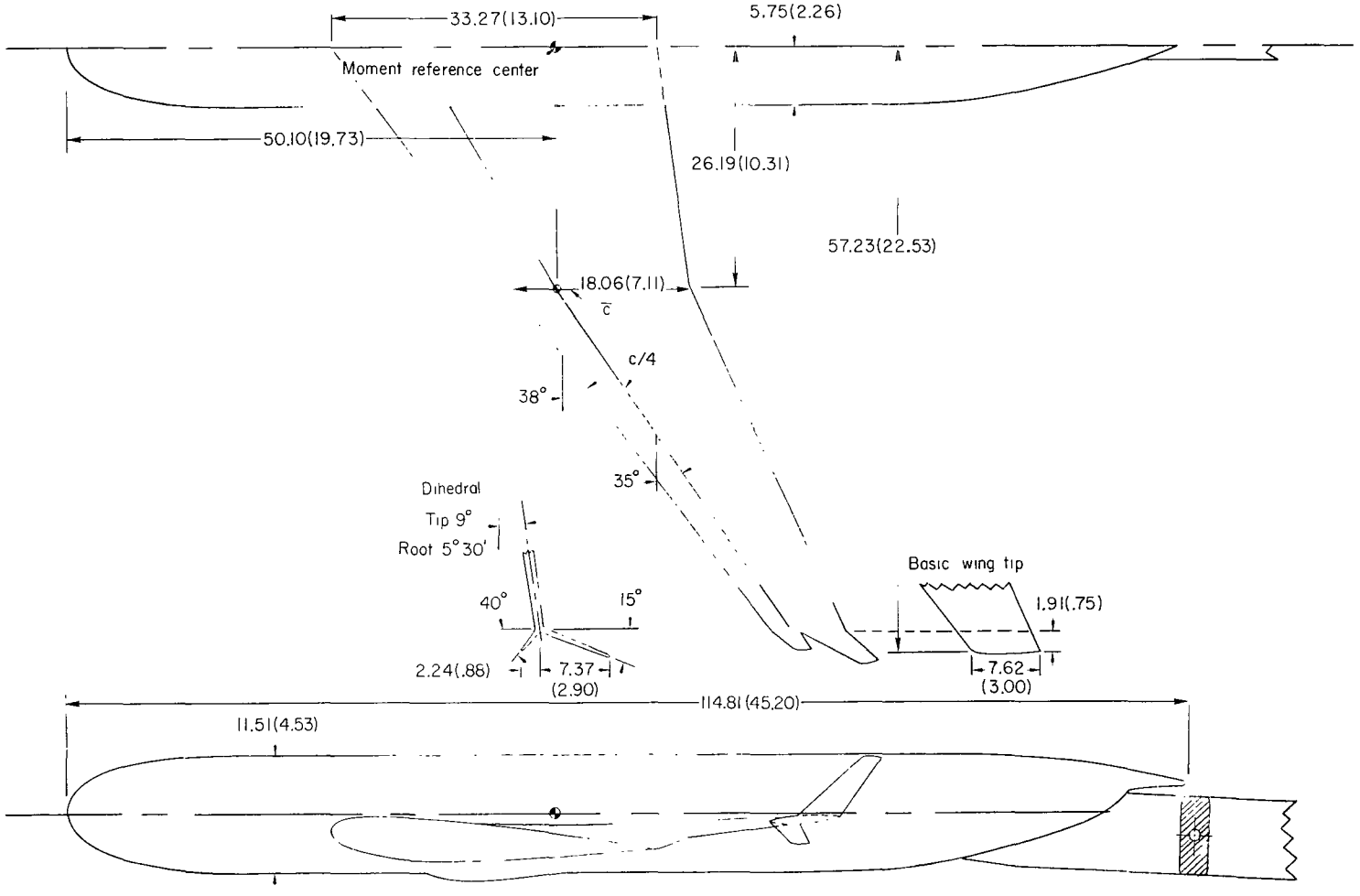

Figure 1.- General arrangement of model. Dimensions are in cm (in.).

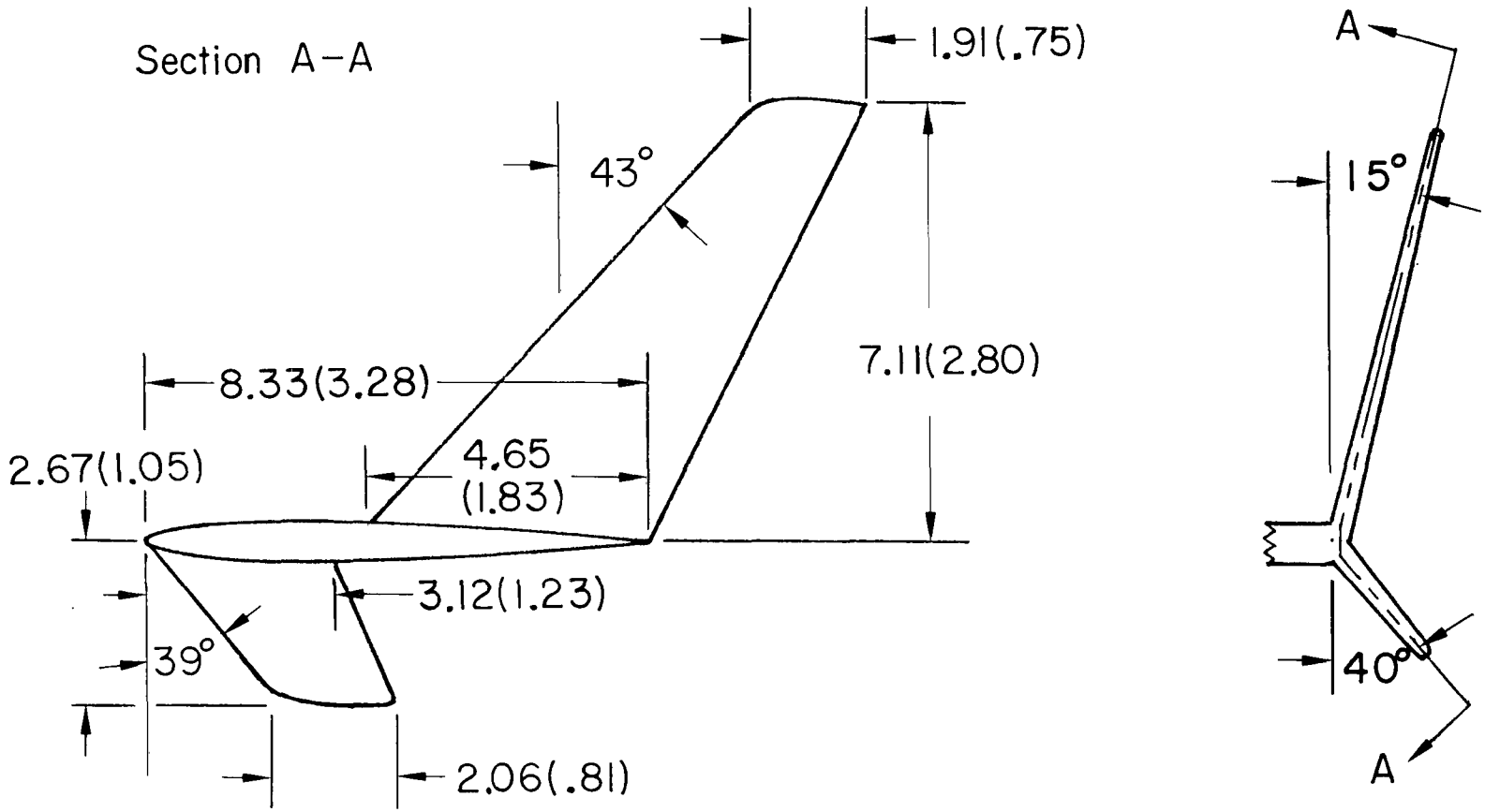

Figure 1.- Concluded.

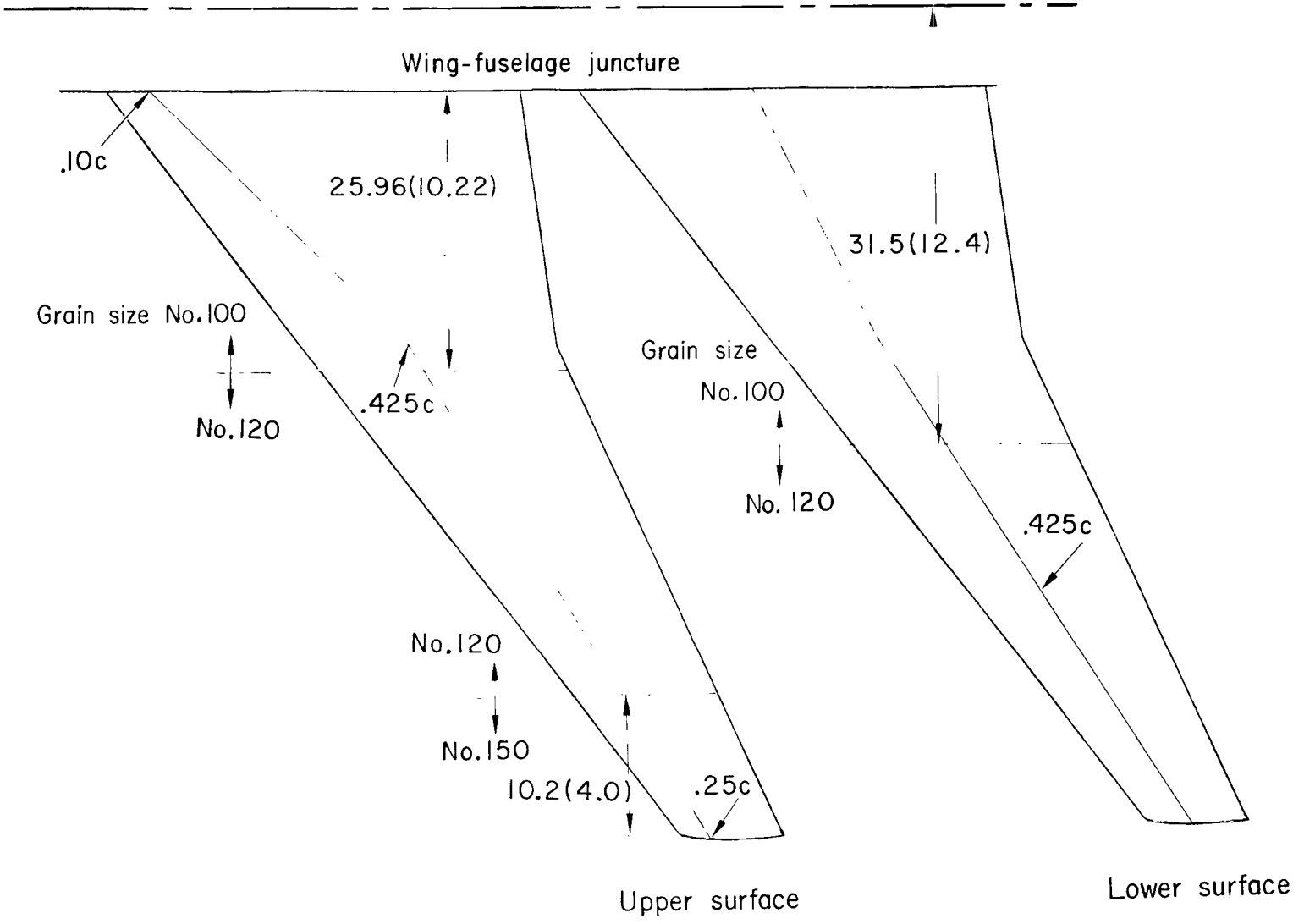

Figure 2.- Location of wing transition strips. Dimensions are in cm (in.).

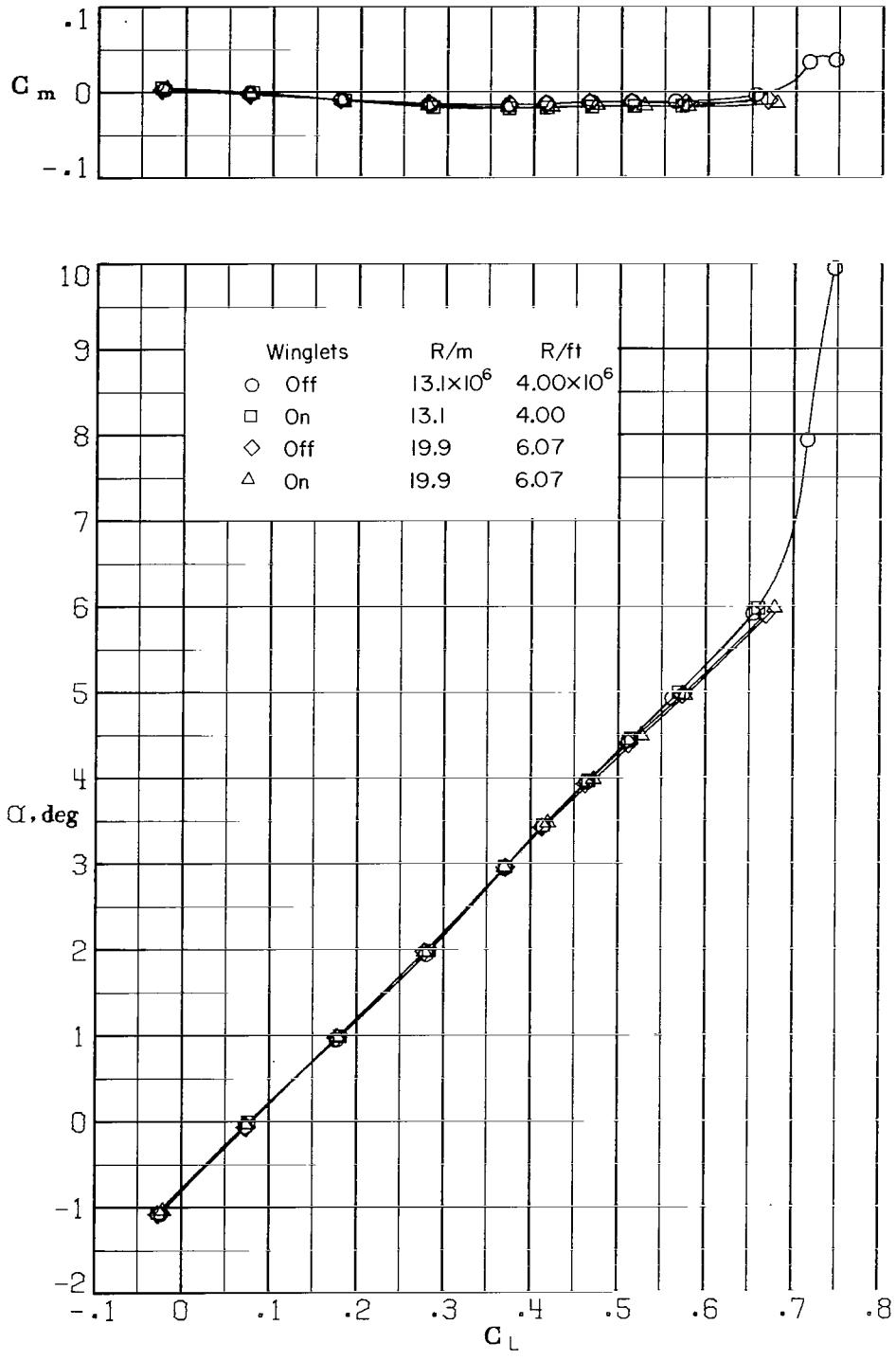

(a) M = 0.750; $\beta = 0^{o}$.

Figure 3.- Variation of pitching-moment coefficient and angle of attack with lift coefficient.

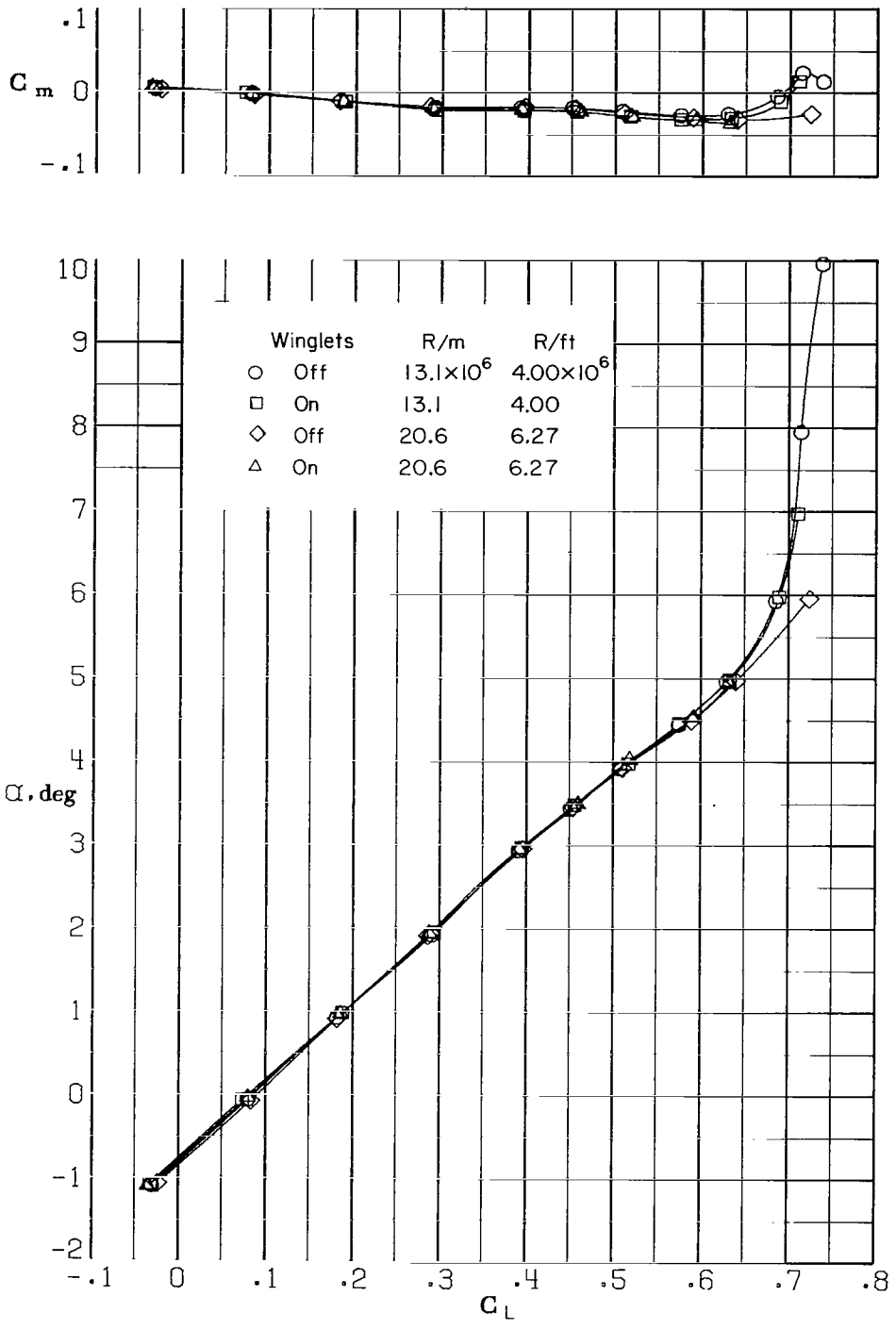

(b) M = 0.800; $\beta = 0^{o}$.

Figure 3.- Continued.

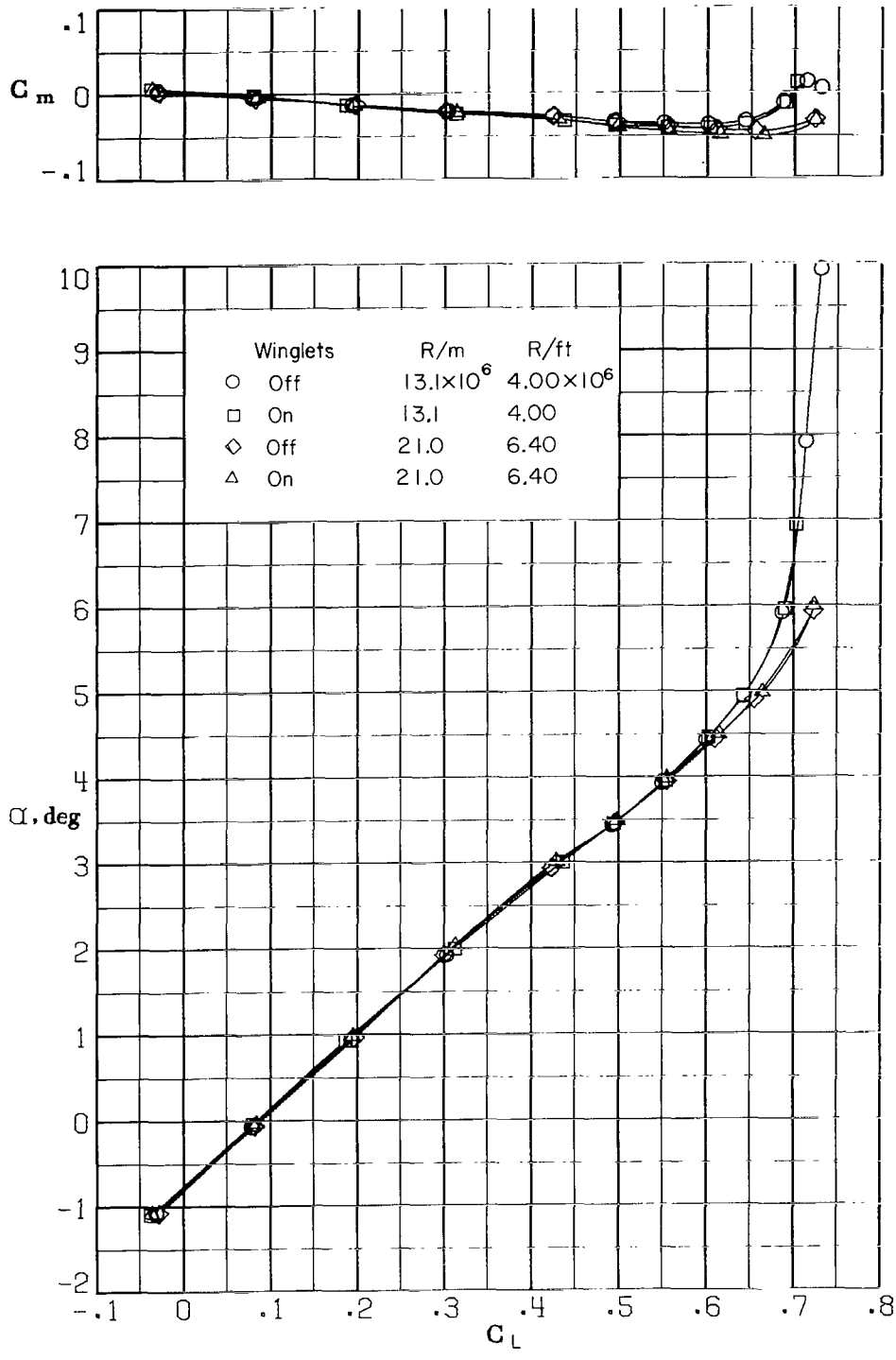

(c) M = 0.825; $\beta = 0^{\circ}$.

Figure 3.- Continued.

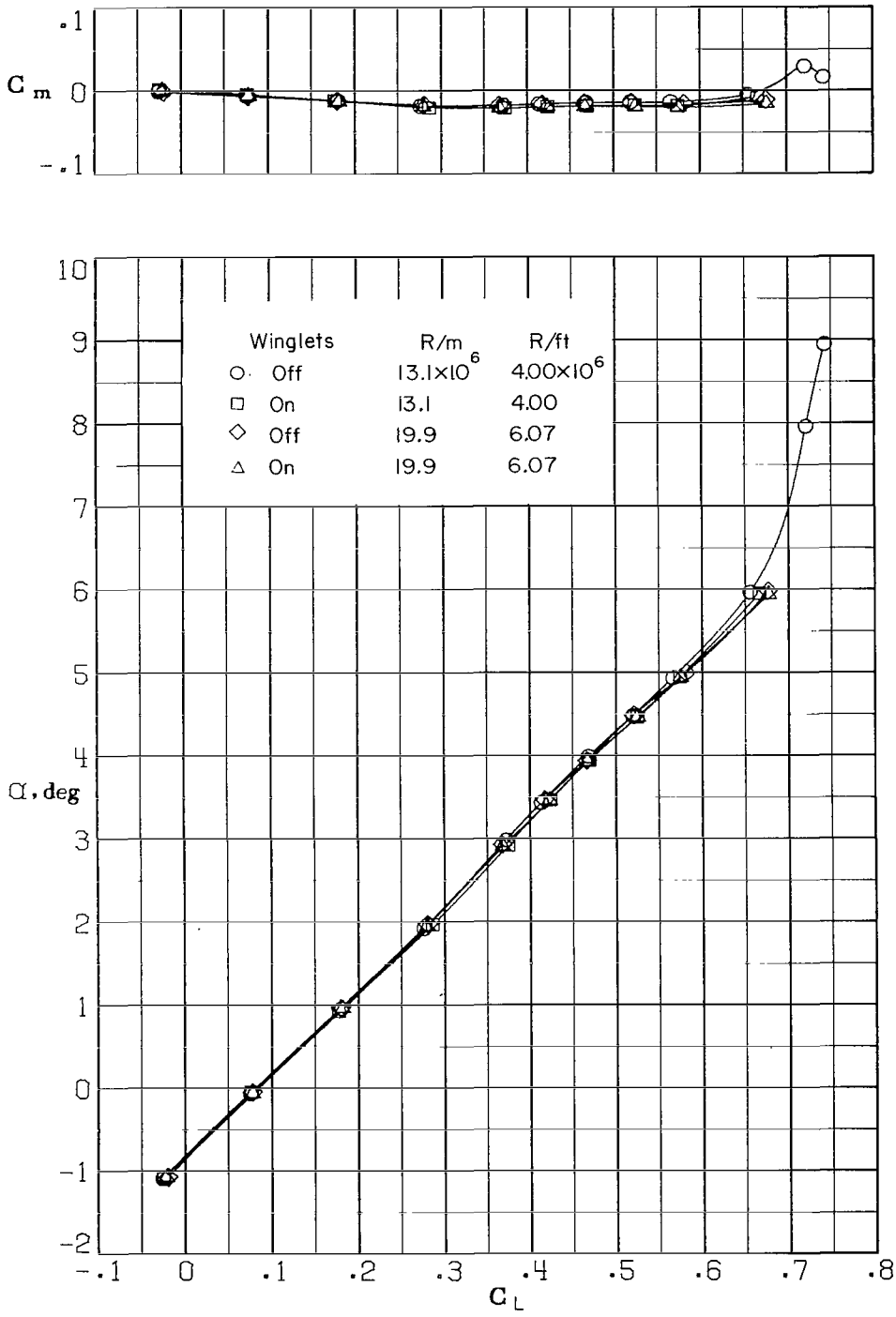

(d) M = 0.750; $\beta = 2.5^{\circ}$.

Figure 3.- Continued.

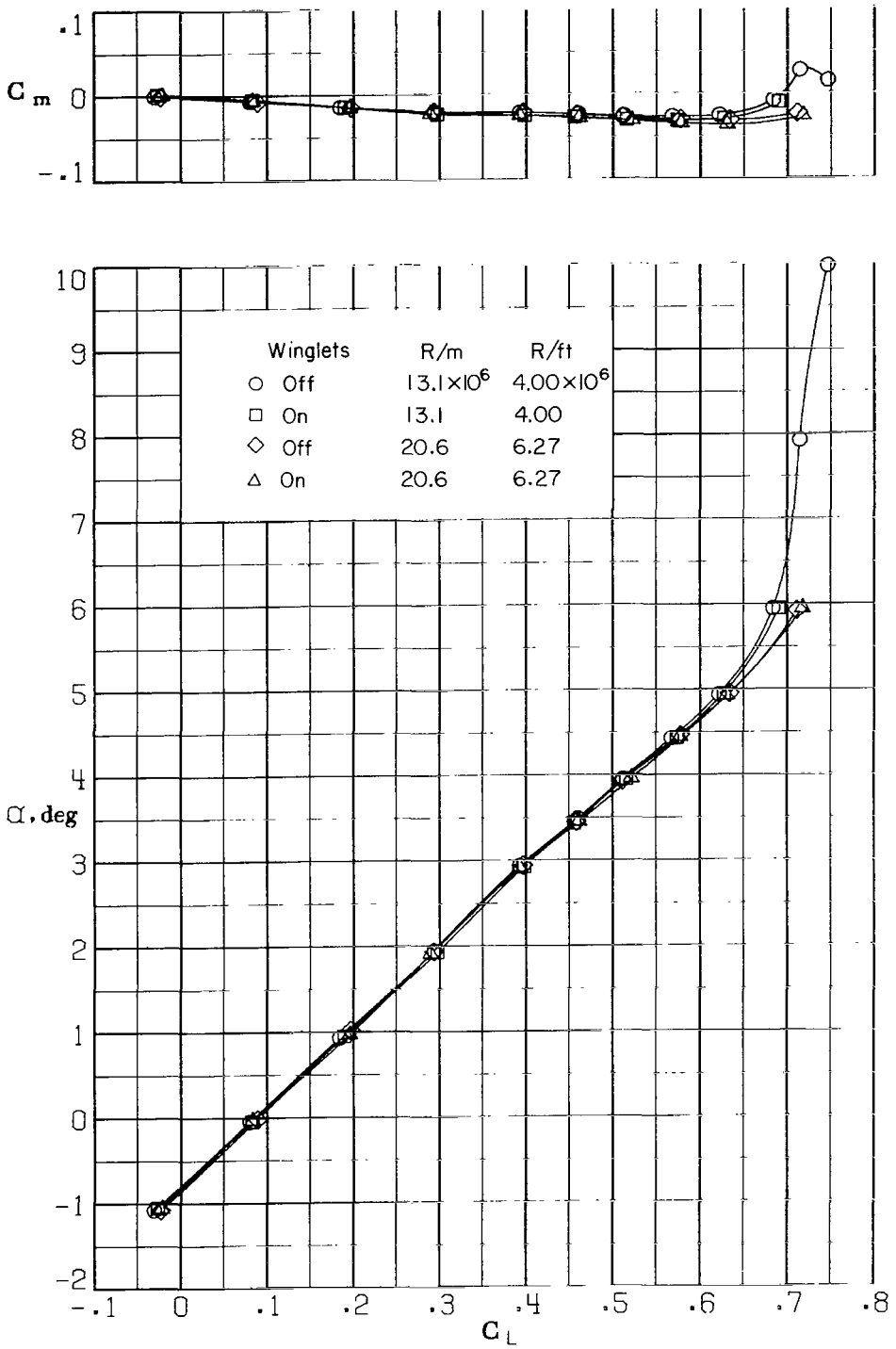

(e) M = 0.800; $\beta = 2.5^{o}$.

Figure 3.- Continued.

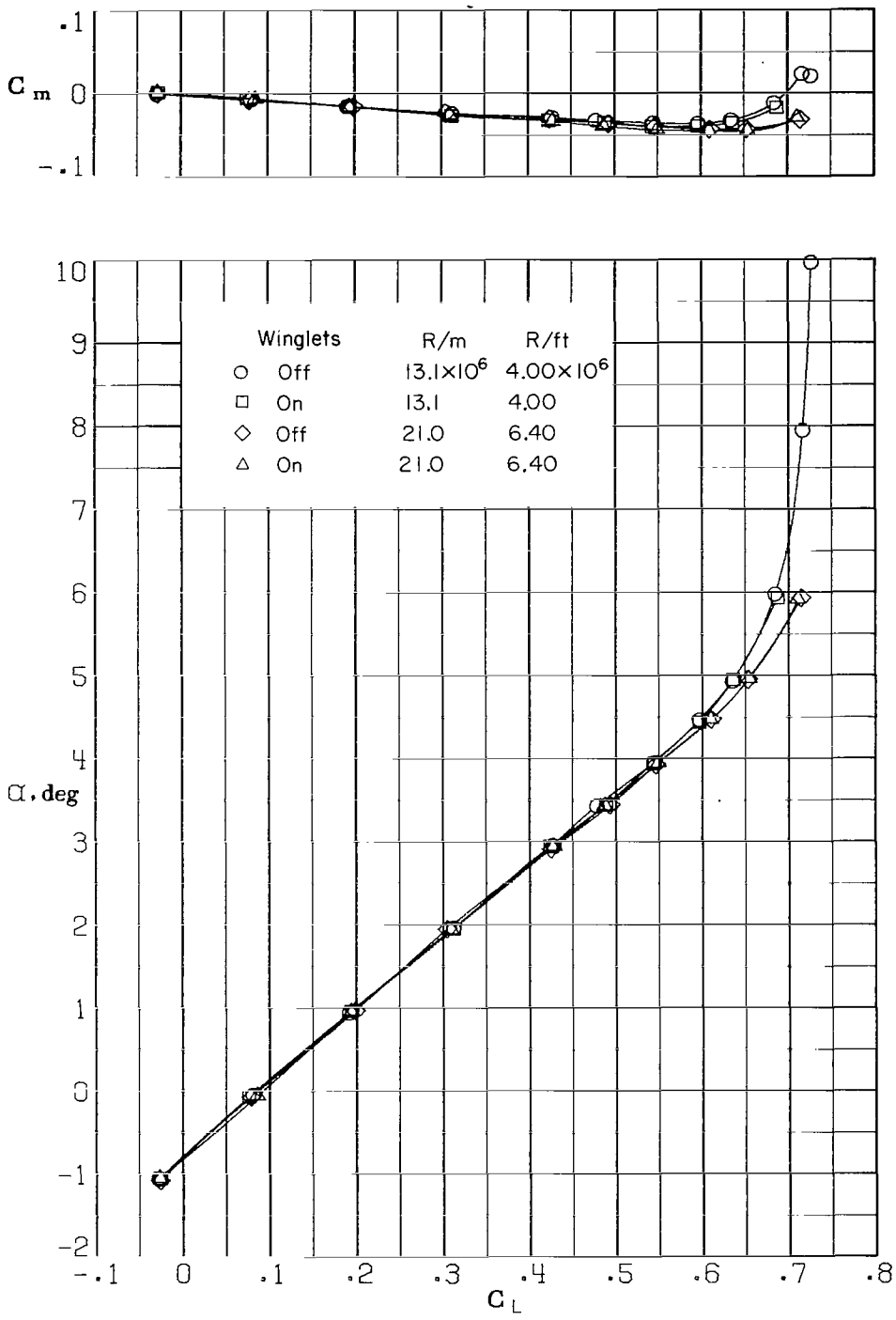

(f) M = 0.825; $\beta = 2.5^{o}$.

Figure 3.- Continued.

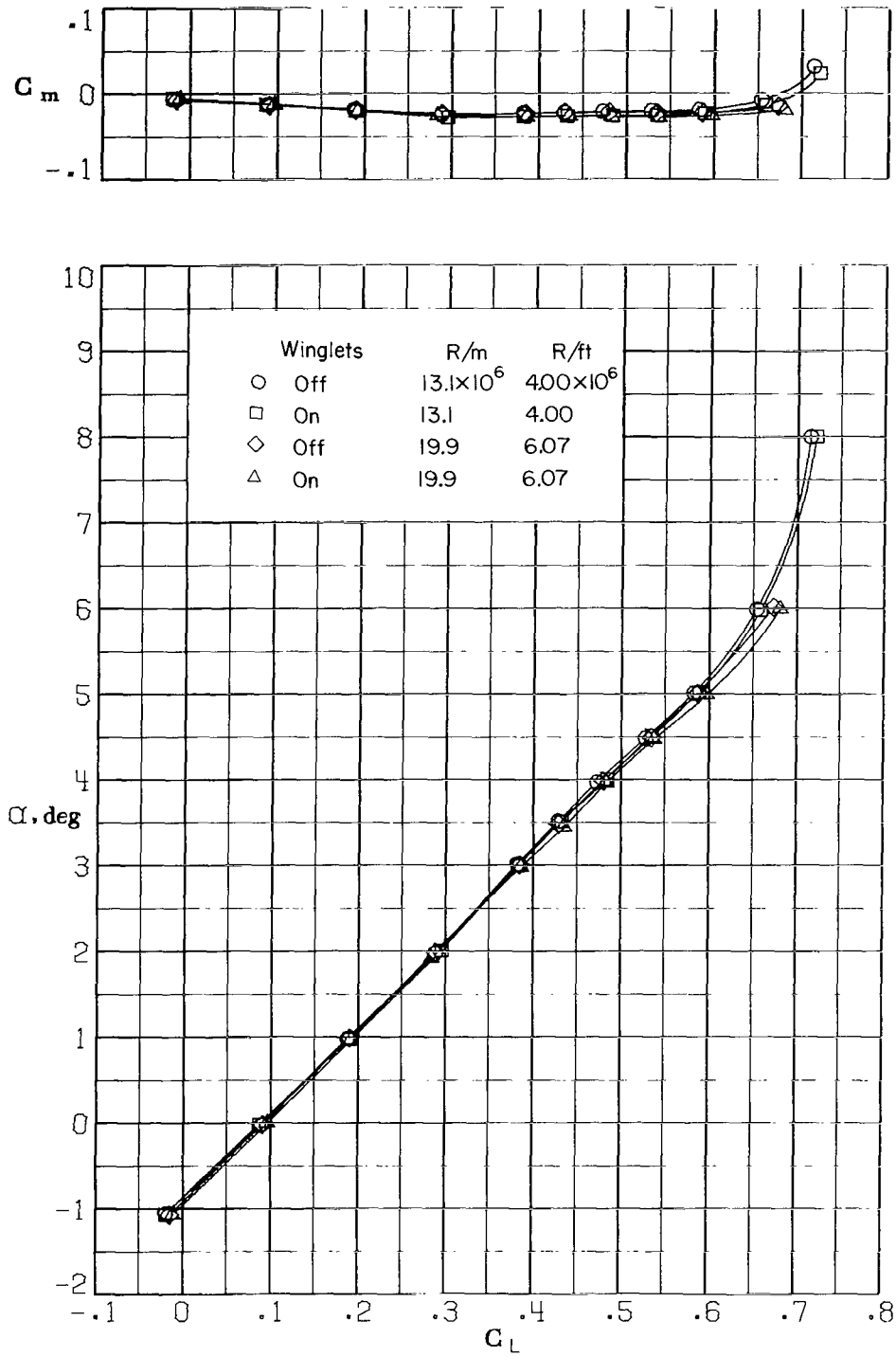

(g) M = 0.750; $\beta = 5^{\circ}$.

Figure 3.- Continued.

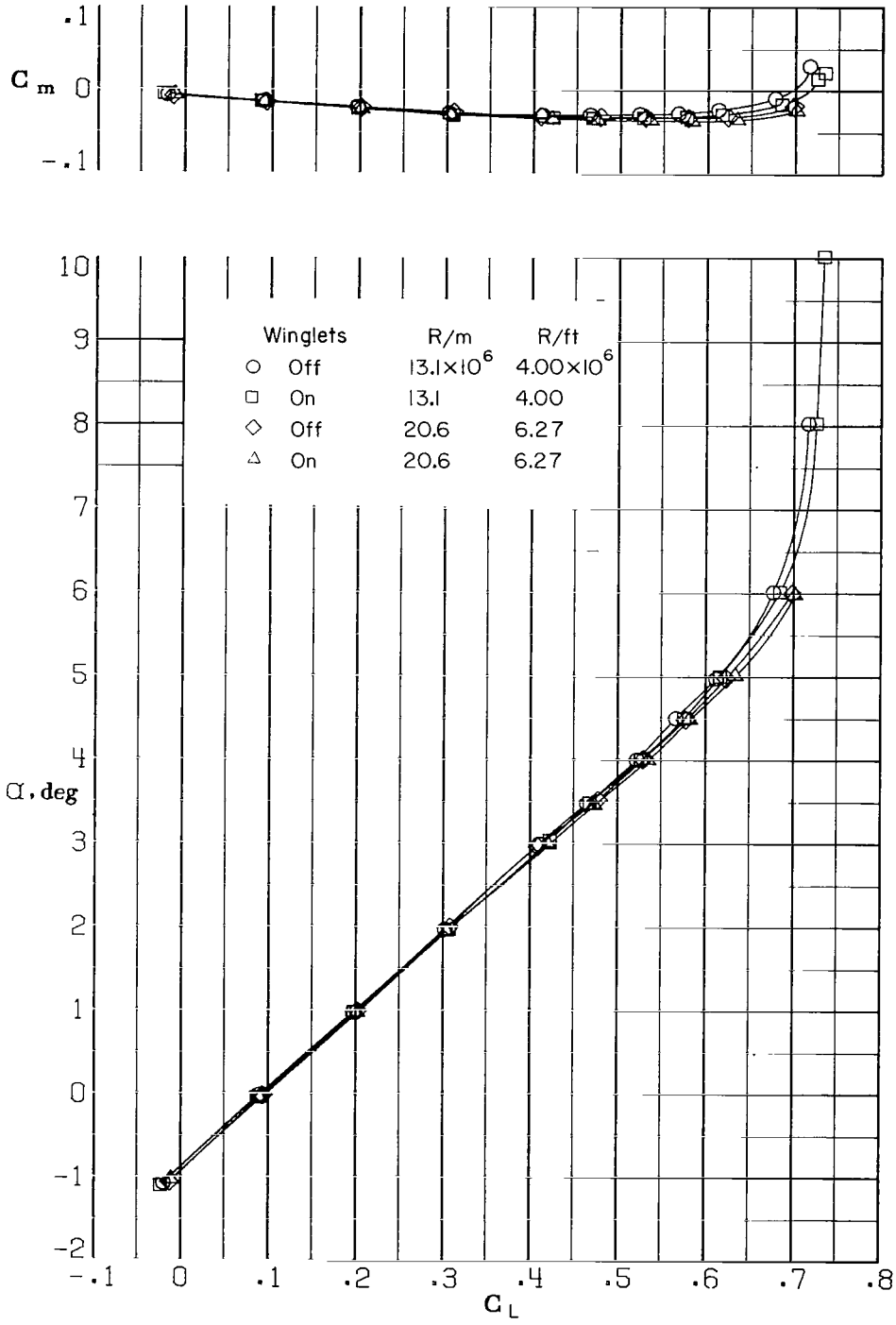

(h) M = 0.800; $\beta = 5^{o}$.

Figure 3.- Continued.

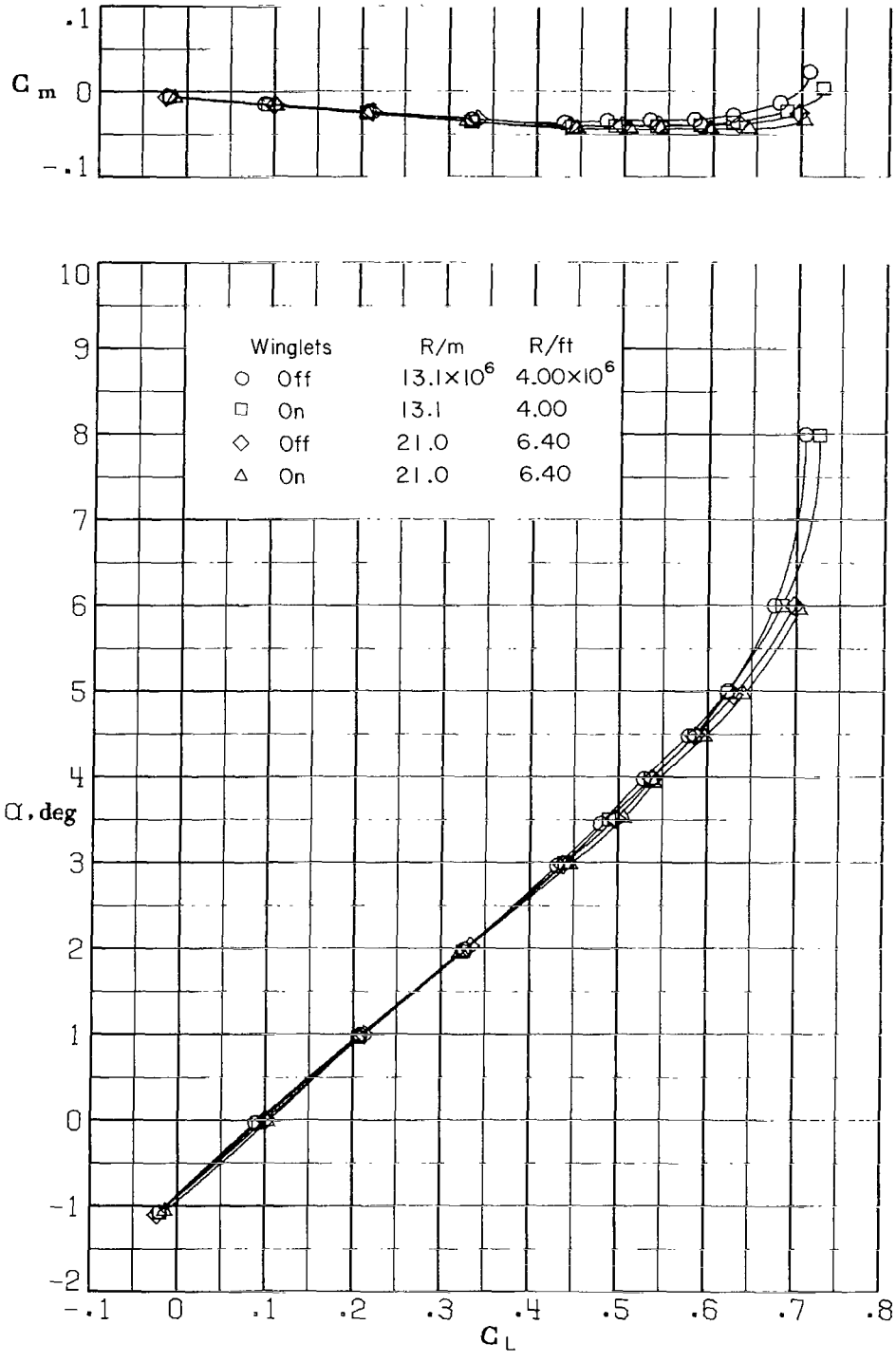

(i) M = 0.825; $\beta = 5^{o}$.

Figure 3.- Concluded.

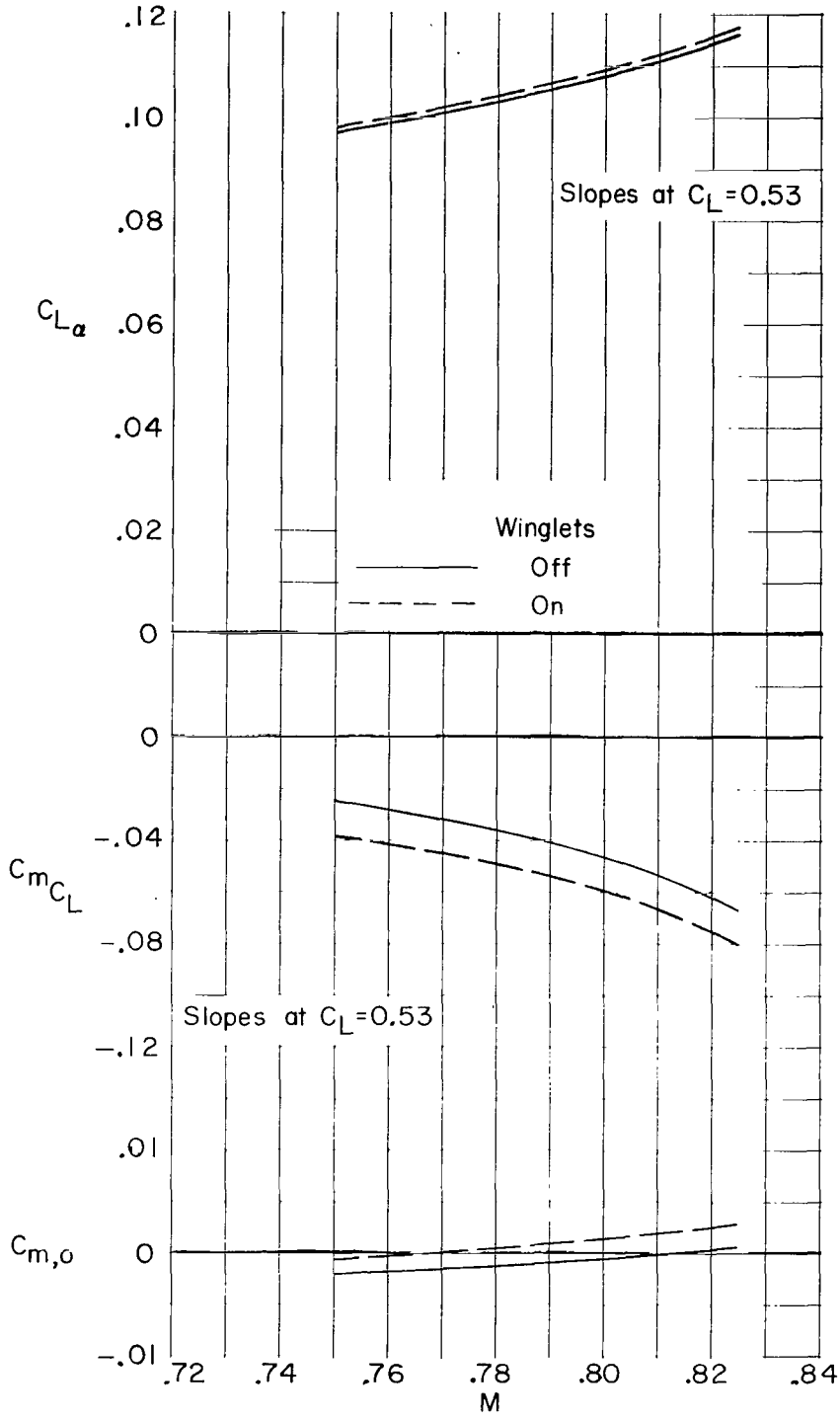

(a) $R \approx 13 \times 10^6$ per meter $(4 \times 10^6$ per foot).

Figure 4.- Summary of static longitudinal aerodynamic characteristics. $\beta = 0^o$.

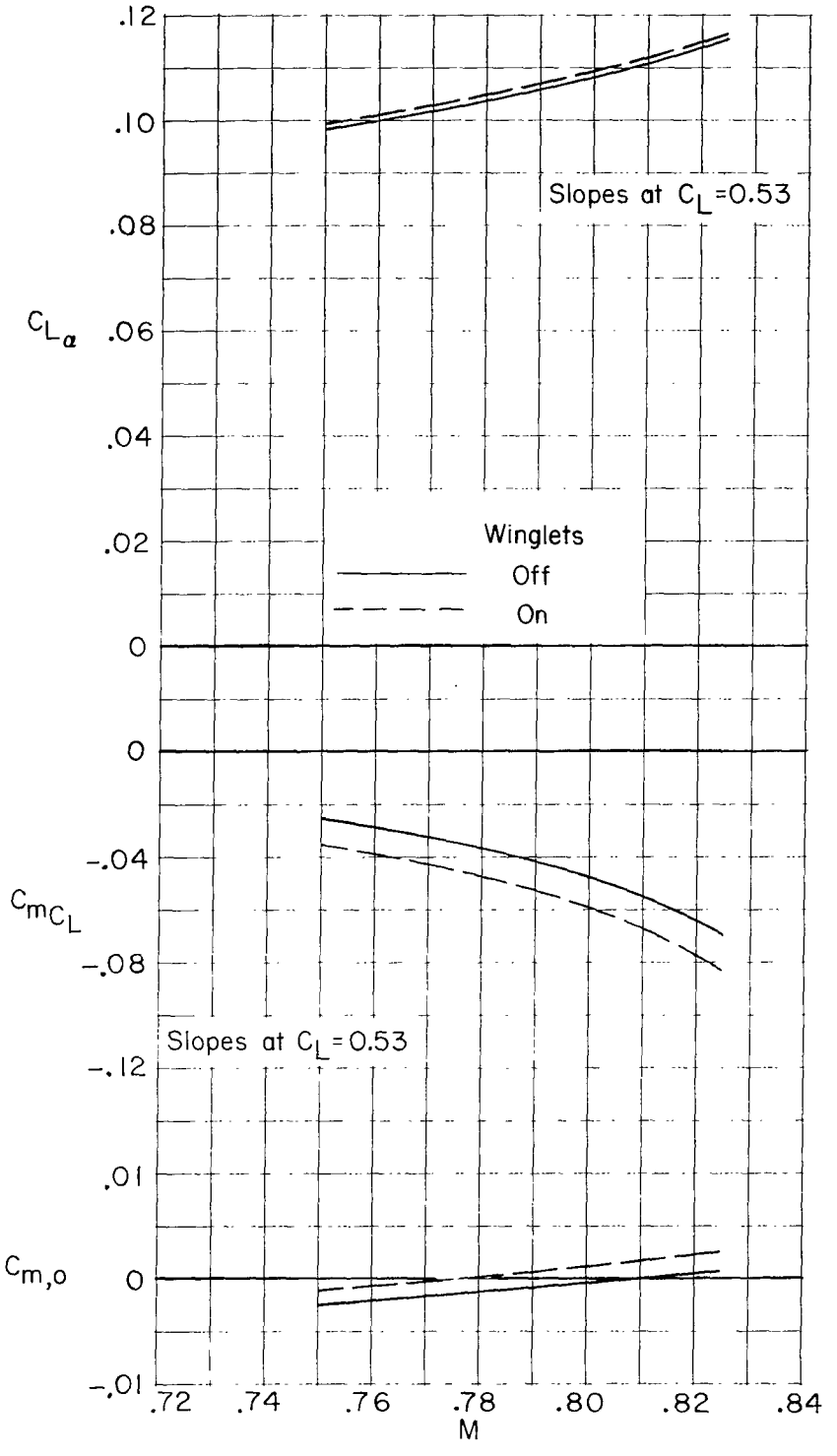

(b) $R \approx 20 \times 10^6$ per meter $(6 \times 10^6$ per foot).

Figure 4.- Concluded.

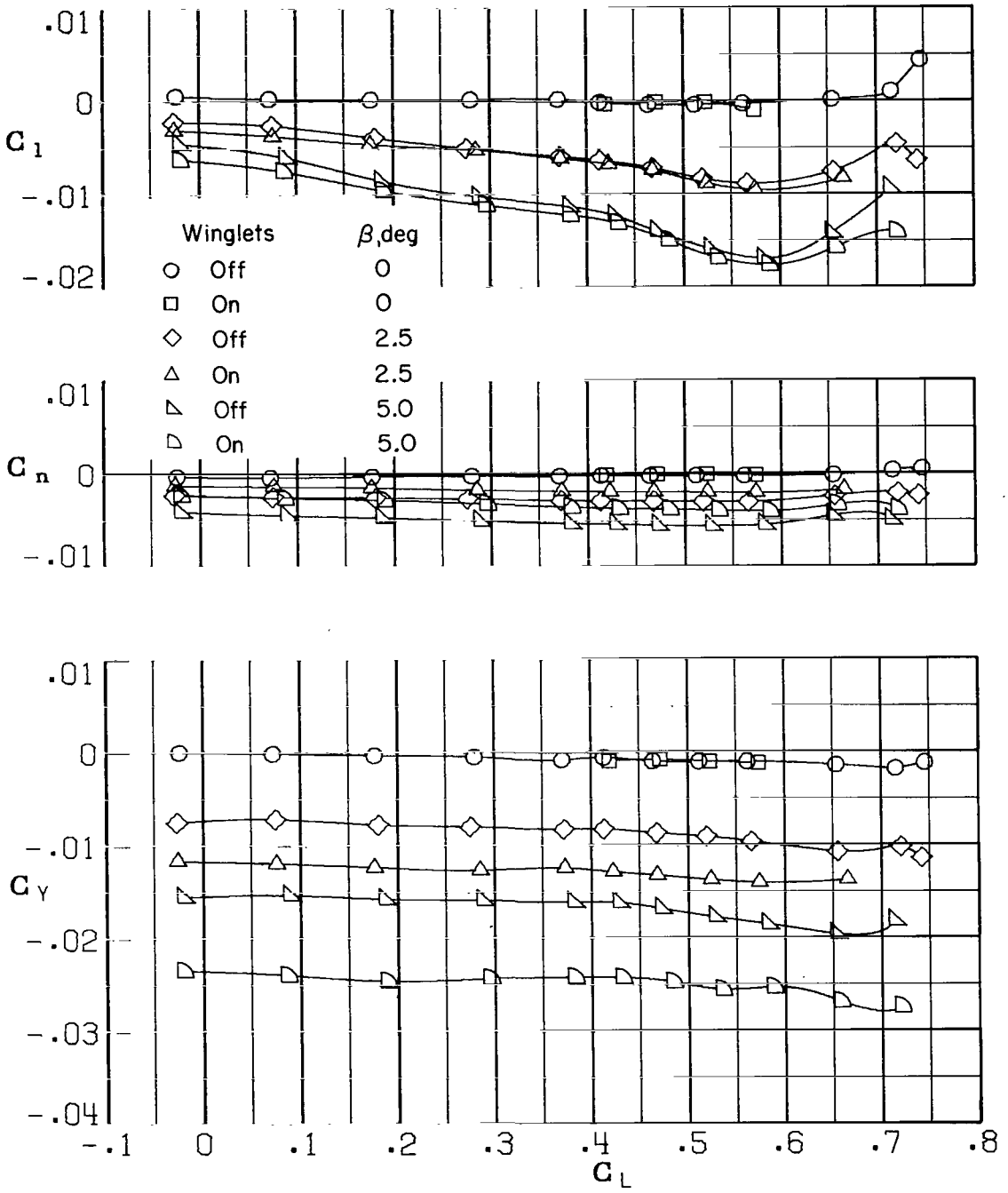

(a) M = 0.750; R ≈ 13×10^6 per meter $(4 \times 10^6$ per foot).

Figure 5.- Variation of rolling-moment, yawing-moment, and side-force coefficients with lift coefficient.

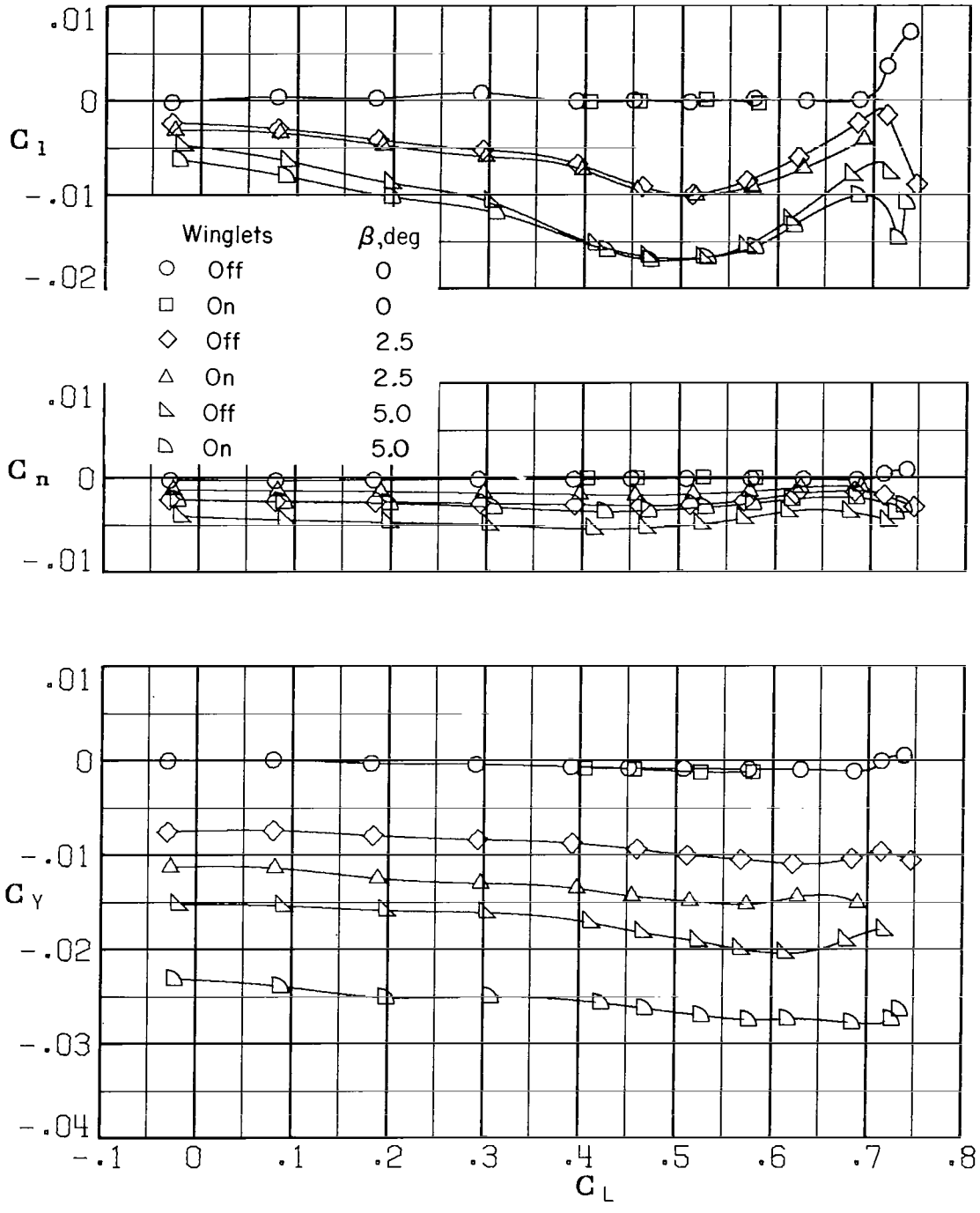

(b) M = 0.80; R ≈ 13×10^6 per meter $(4 \times 10^6$ per foot).

Figure 5.- Continued.

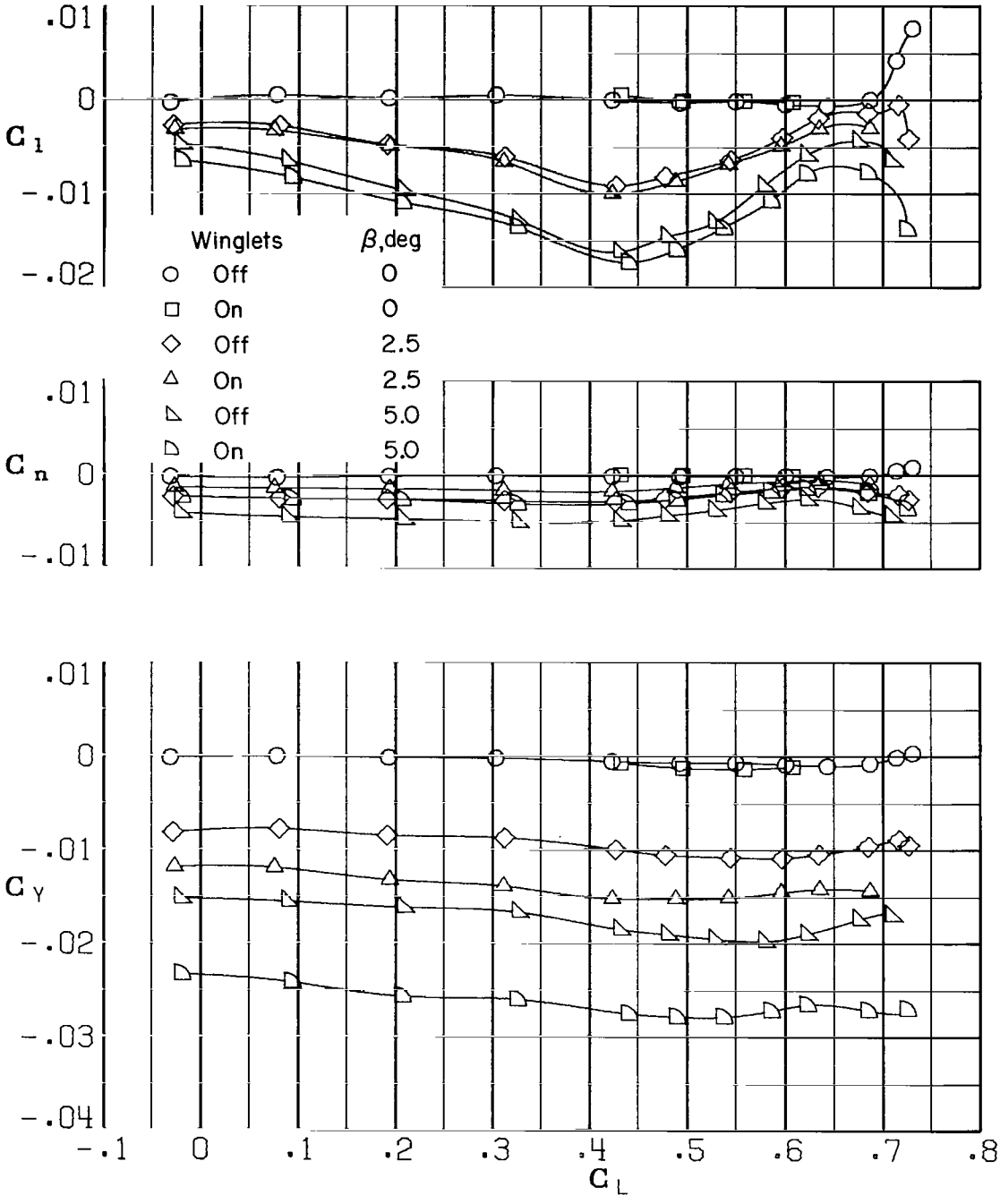

(c) M = 0.825; R ≈ 13×10^6 per meter $(4 \times 10^6$ per foot).

Figure 5.- Continued.

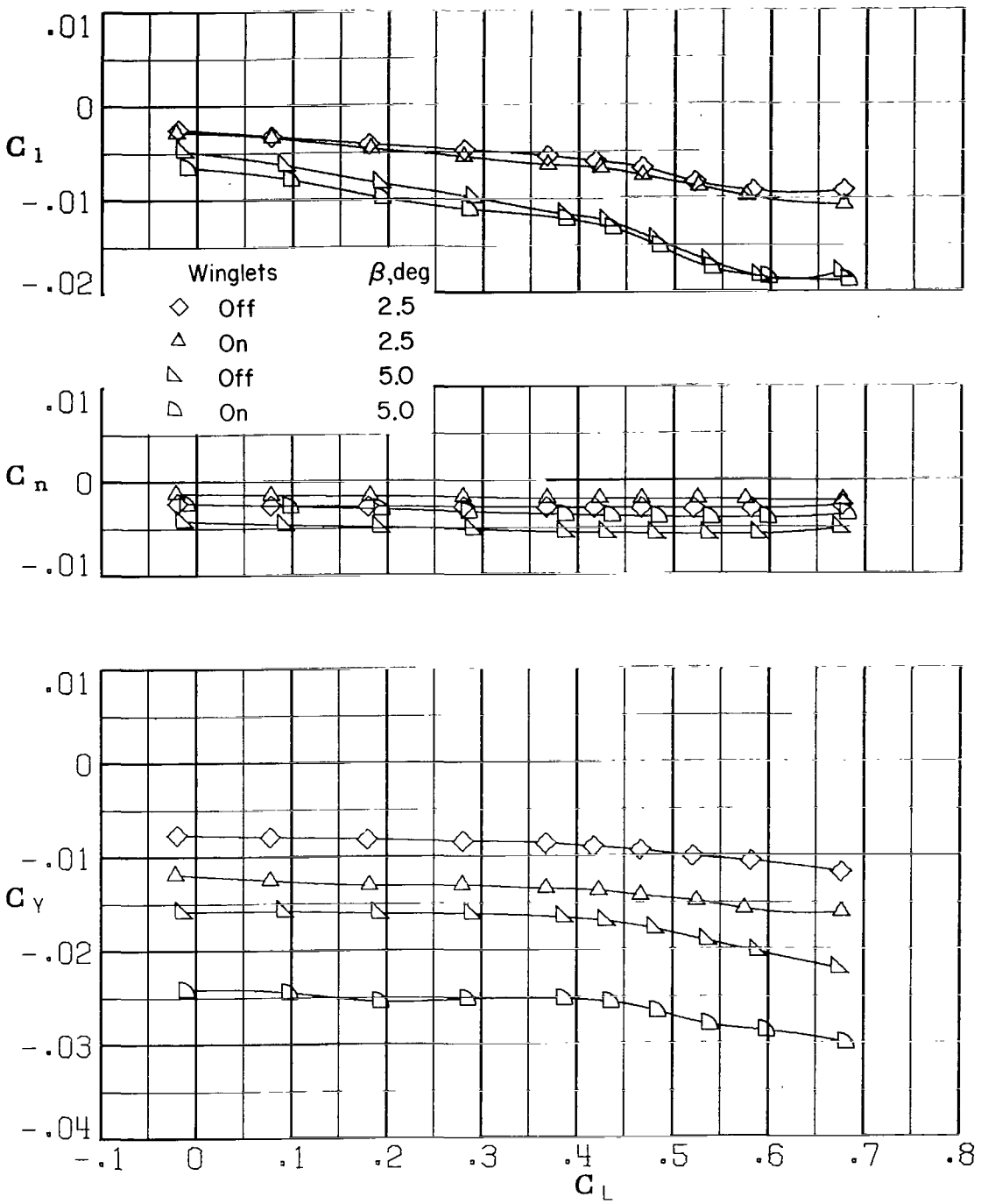

(d) M = 0.750; R ≈ 20×10^6 per meter $(6 \times 10^6$ per foot).

Figure 5.- Continued.

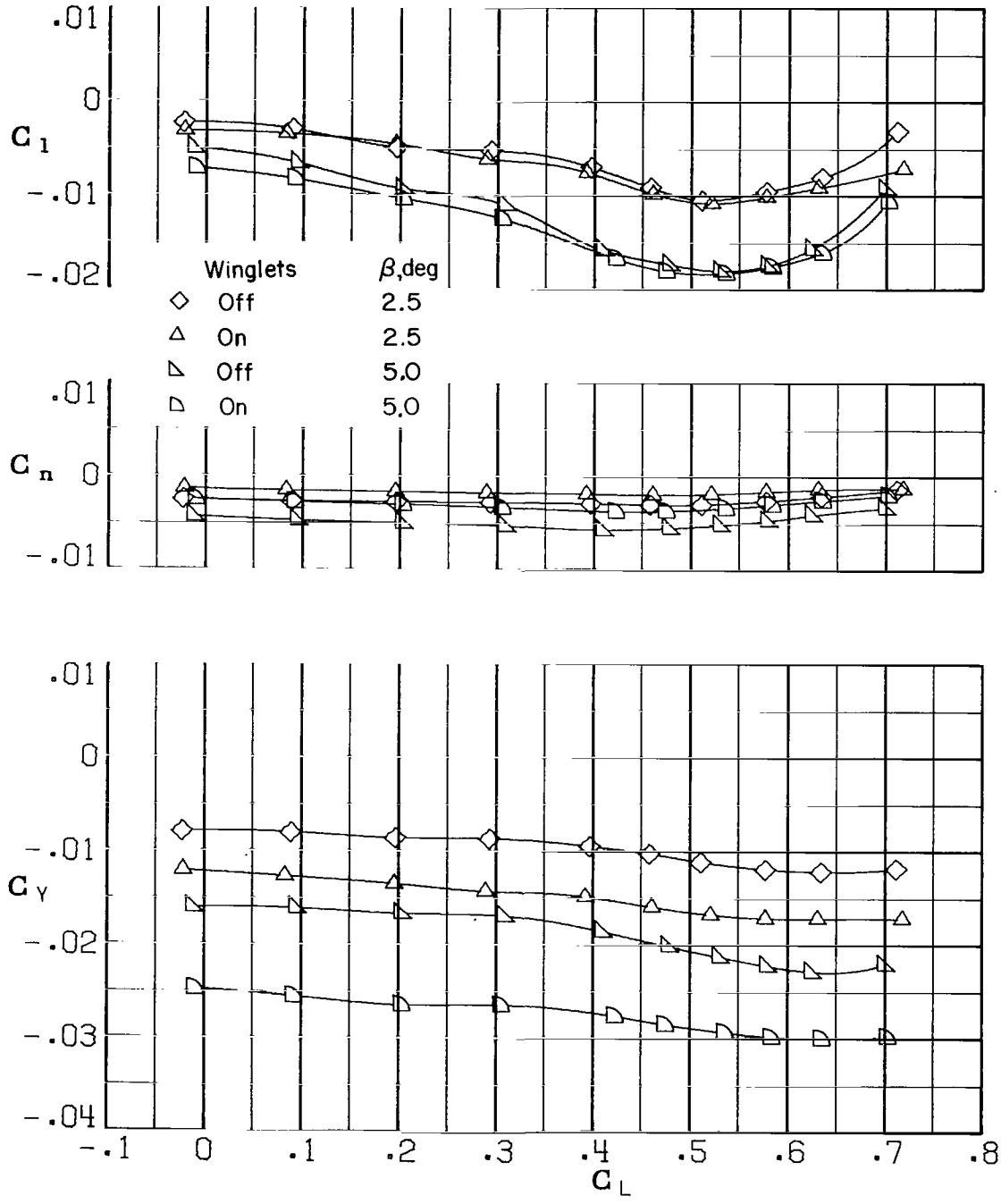

(e) M = 0.80; R ≈ 20×10^6 per meter $(6 \times 10^6$ per foot).

Figure 5.- Continued.

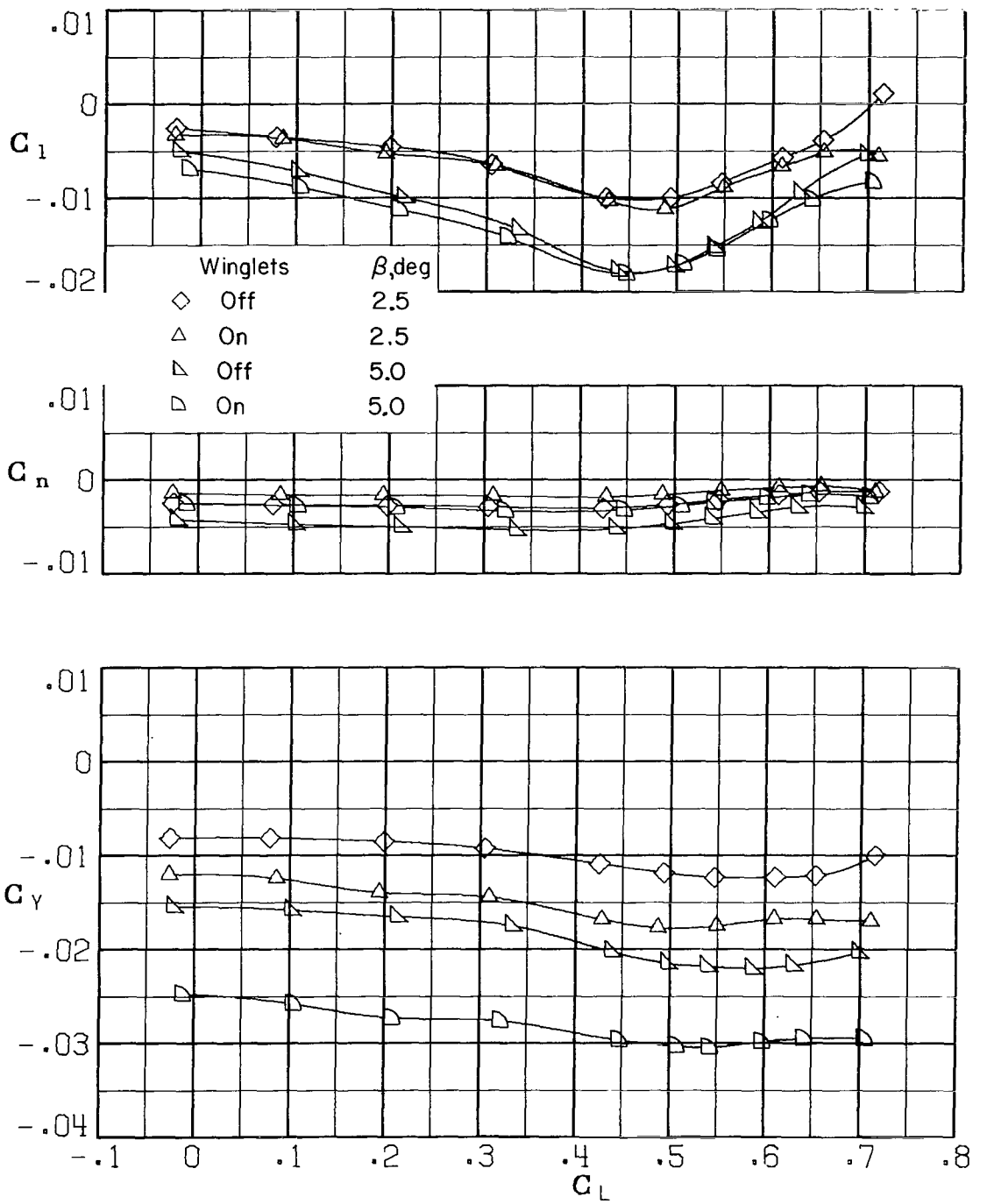

(f) M = 0.825; R ≈ 20×10^6 per meter $(6 \times 10^6$ per foot).

Figure 5.- Concluded.

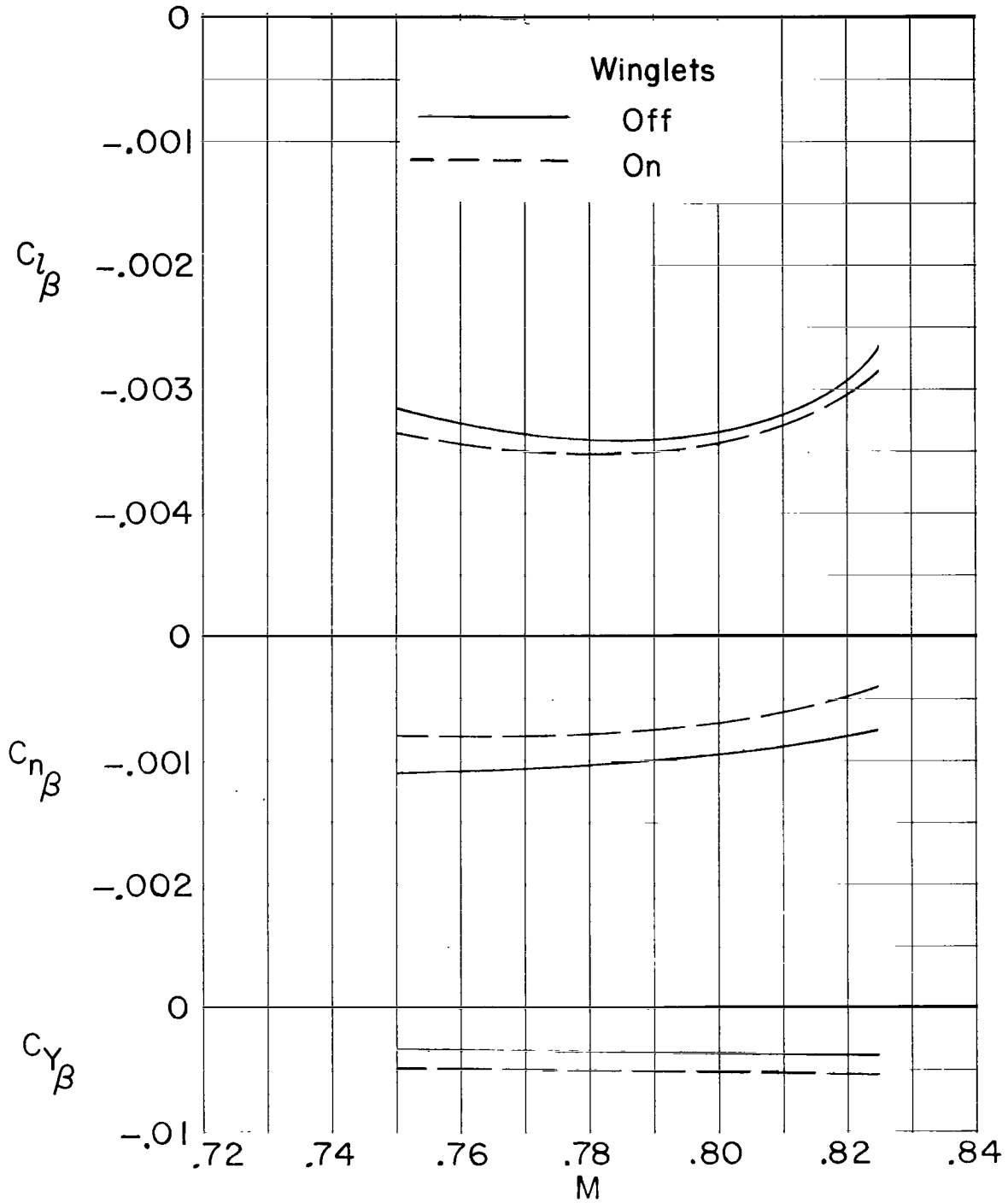

(a) $R \approx 13 \times 10^6$ per meter $(4 \times 10^6$ per foot).

Figure 6.- Summary of static lateral aerodynamic characteristics. $C_L = 0.53$.

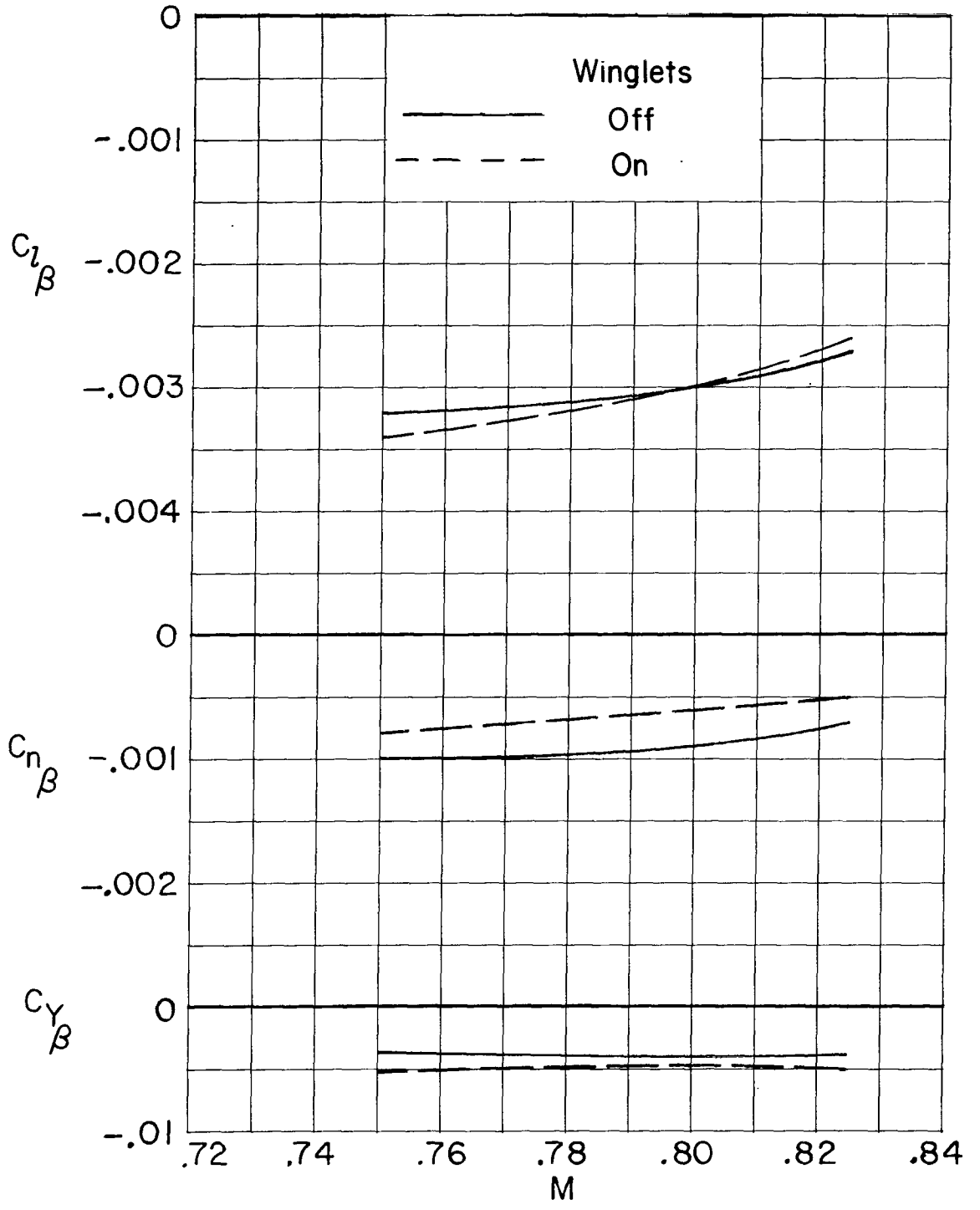

(b) $R \approx 20 \times 10^6$ per meter $(6 \times 10^6$ per foot$)$.

Figure 6.- Concluded.

NASA-Langley, 1976 L-10297